Preparation and Properties of Thin Films of Hyperbranched Polyesters with Different End Groups

Detlev Beyerlein[a], Georg Belge[b], Klaus-J. Eichhorn[a]*, Günter Gauglitz[b], Karina Grundke[a], Brigitte Voit[a]

[a] Institut für Polymerforschung Dresden e.V., Hohe Straße 6, 01069 Dresden, Germany

[b] Universität Tübingen, Institut für Physikalische Chemie, Auf der Morgenstelle 15, 72076 Tübingen, Germany

Summary: Hyperbranched polyesters (HBP) with different end groups were prepared as thin films. They were characterized with regard to their chemical composition, thickness, optical constants and morphology using infrared spectroscopy, spectroscopic ellipsometry, and atomic force microscopy. The surface properties of the films were determined by zeta-potential and contact angles measurements. The differences in the molecular structure and surface energetic and acid-base properties between HBP materials with carboxylic, hydroxy and acetoxy end groups result in differences in their swelling behavior in atmospheric humidity. The swelling behavior at different atmospheric humidity was observed in situ using spectroscopic ellipsometry and reflectometric interference spectroscopy. From the results it can be concluded that HBP films can be used potentially as sensoric materials.

Introduction

There is a strong interest in hyperbranched polymers with the main fields of applications being discussed in blends, coatings or resins, or as additives[1)]. However, especially thin films of hyperbranched polymers similarly prepared on solid surfaces like perfect dendrimers might be useful also as materials for chemical sensors or as diagnostic tools, because of their high number of functional groups and the interesting branched architecture. Recently, Crooks, Bergbreiter, Bruening and coworkers started to work in this field of application of thin films of dendritic polymers[2)]. The investigations were focused particularly to surface immobilized dendrimer layers, which were often terminated with acid and amino groups. Thus, Tokuhisa and Crooks reported interactions between organized, surface-confined dendrimer monolayers and vapor-phase probe molecules[3)]. Their poly(aminopropane-1,3-diyl) dendrimers with different amine and amide terminal groups were covalently linked to a Self-Assembled Monolayer (SAM) modified gold surface. The sensitivity and selectivity to Volatile Organic Compounds (VOC) were studied by the Surface Acoustic Wave (SAW) technique. In an other work[4)] poly(amidoamine) (PAMAM) dendrimer monolayers and dendrimer-alkane thiol mixed monolayers adsorbed on gold were evaluated. All this dendrimer layers are very thin

 CCC 1022-1360/00/$ 17.50+.50/0

(thickness 1-5 nm) and covalently linked to the substrate. The synthesis of the applied perfectly branched dendrimers and the preparation and characterization of the monolayers as well are difficult and expensive. Thus highly functionalized "dirty" imperfect hyperbranched polymers (HBP) prepared in a one-step synthesis could be an interesting alternative. A possibility of hyperbranched poly(acrylic acid) linked to the surface is pointed out by Bruenning et al.[5] The material is still build up in several steps by grafting from the surface. It should also be possible to graft onto a surface.

According to Tokuhisa et al.[6] polymeric layers should be sufficiently thin that permeation transients are avoided but thick enough for a good sensitivity. That means that the layer should be thicker than monolayer (some Å) and thinner than often applied well known sensor layer made from amorphous polymers (1-2 μm). For that reason we prepared thin films of several hyperbranched polyesters having hydroxyl, carboxyl and acetoxy end groups by spin-coating on silicon wafers or glass substrates. Spectroscopic ellipsometry was used to determine the thickness and optical constants of the films. The morphology of the films was studied by optical and atomic force microscopy. The chemical composition was characterized by FTIR spectroscopy. Zeta-potential and contact angle measurements based on axisymmetric drop shape analysis were carried out to characterize the acid-base properties and the surface free energies of the polymer surfaces.

To demonstrate the potential as sensor material we present our first results on the swelling and/or adsorption/desorption properties of these films by variation of the atmospheric humidity. Recently, Bielsaski and Rühe[7] presented an experimental study on the swelling of thin polymer layers in humid air. They investigated the interactions of covalently attached polyelectrolyte brushes with water as function of humidity by Optical Waveguide Spectroscopy (OWS). Changes in thickness and refractive index due to the swelling of their several hundred nm thick films were measured as sensoric response.

In the following study on thin HBP films we used dynamic spectroscopic ellipsometry and Reflectometric Interference Spectroscopy (RIfS) to follow the swelling processes *in situ*.

Materials and methods

Hyperbranched polymers (HBP)

This study includes three hyperbranched polyesters (HBP) with the same backbone structure but different end groups synthesized by Schmaljohann[8]. The polyester are prepared by melt polycondensation of AB_2 monomers 3,5-trimethylsiloxyl benzoyl chloride, 3,5-diacetoxy benzoic acid, and 5 acetoxyphthalic acid, respectively. Fig. 1 and Table 1 show the structure

and some analytical data of our HBP. Further details on synthesis and properties can be found elsewhere.[8,9)]

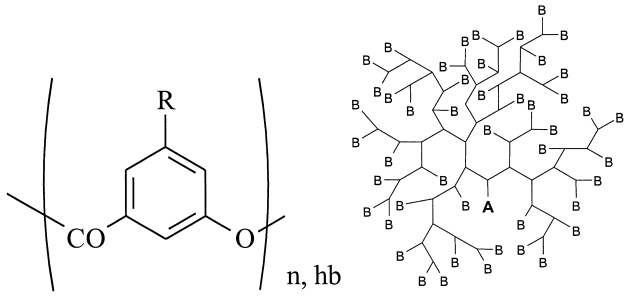

Fig. 1 Chemical structure of HBP (R=B)

Table 1 Properties of the synthesized HBP[8)]

Terminal group R	name of HBP	M_W [g/mol]	T_g [°C]	Degree of Branching	water content [%]
-OH	P-OH	16,000	220	0.60	1.9
-COOH	P-COOH	15,500	235	n.d.	2.1
$-OCOCH_3$	P-OAc	13,500	155	0.50	0.3

Preparation of thin HBP layers

Silicon wafers with a thermal oxide layer of about 50 nm (SilChem) were used as substrates. After cleaning by rinsing with water (Millipore), acetone, and water, they were flushed with dry N_2.

Glass substrates with 10 nm Ta_2O_5 and 330 nm SiO_2 (Schott) were used for the RIfS. Before coating they were emerged in a piranha solution (H_2O_2 (30%, Merck) / H_2SO_4 (98%, Merck) 1:4) and treated 15 min with ultrasonic.

A 2% (w/w) solution of HBP in tetrahydrofurane (Merck, distilled) was used for spin casting (30 seconds, 2000 rpm). Heating above T_g for 1 hour removed the solvent and smoothed the coatings (annealing temperatures: P-OH, P-COOH 240°C, P-OAc 180°C). For the zeta-potential and the contact angle measurements also samples without annealing were used. In this case they were stored over night in vacuum at room temperature to remove the solvent.

Spectroscopic ellipsometry

The thickness and the optical constants of the HBP films have been determined using a rotating analyzer type variable angle multiwavelength ellipsometer M-44 (Woolam Co., Inc). The

ellipsometric data Δ and Ψ were measured simultaneously at 44 discrete wavelengths (428.0 – 763.5 nm) and three angles of incidence (65°, 70° and 75°)[10]. In the fitting procedure, an optical two-layer model was used: Si-substrate/SiO_2-layer/HBP-layer/air. The optical constants for Si and SiO_2 were taken from the literature. As in previous studies on polymer layers,[10,11] a Cauchy function was successfully applied to describe the wavelength dependence of the refractive index n.

All ex-situ measurements were performed at 22 °C and 40-50 % relative humidity.

Atomic Force Microscopy (AFM)

The topography of the film surfaces has been quantified by AFM. The experiments were performed in tapping mode under ambient conditions using a Nanoscope IIIa BioScope from Digital Instruments, Santa Barbara. Height images for roughness measurements were recorded in soft tapping mode. A three dimensional roughness parameter, S_a, was calculated giving an average over the whole surface area.

Infrared spectroscopy

Functional groups were investigated by transmission FTIR spectroscopy with a IFS 66V (Bruker) equipped with a MCT detector. A pure Si-wafer was measured for the background spectra. All spectra cover the range from 4000 to 600 cm^{-1}.

The separation of bands is realized with the Opus/IR menu fit curves (Bruker).

Zeta potential measurements

To characterize the surface properties of the bare and coated silicon surfaces by zeta potential measurements the Electrokinetic Analyzer EKA of Anton Paar KG, Austria, was applied using a measuring cell suitable for macroscopic sheets. A pair of bare or coated silicon wafers are placed in such a way that a capillary slit is formed with a cross-section area. After creating a hydrostatic pressure an electrolyte solution ($3 * 10^{-4}$ mol/l KCl) is streaming through this slit. By shearing the diffuse part of the electrical double layer at the solid/liquid interfaces the difference in the electrical potential ΔU can be measured by means of Ag/AgCl electrodes. From the quotient of the potential and the pressure difference the zeta potential ζ of the shear plane can be calculated using the Helmholtz-Smoluchowski-equation. From the zeta potential vs. pH of the electrolyte solution information about the acid-base character of the solid surface is obtained[12].

Contact angle measurements using axisymmetric drop shape analysis (ADSA)

Axisymmetric drop shape analysis-profile (ADSA-P) was used to measure advancing and receding contact angles. ADSA-P is a technique to determine liquid-fluid interfacial tensions and contact angles from the shape of axisymmetric menisci, i.e., from sessile as well as pendant drops. The strategy employed is to fit the shape of an experimental drop to the theoretical drop profile according to the Laplace equation of capillarity. Details of the methodology can be found in[13]. Computer software has been developed to implement this method and computational results provide simultaneously the values of interfacial tension, drop volume, surface area, contact angle and the radius of the three-phase contact line[14]. A SUN workstation was used to acquire images from the image processor and to perform the image analysis and computation. The accuracy of measured contact angles obtained by the ADSA technique (± 0.3°) is an order of magnitude better compared to the frequently applied conventional goniometer sessile drop technique (± 2-3°)[15].

Reflectometric Interference Spectroscopy (RIfS)

The glass substrates are irradiated with light from the backside. The light passing through the layers and some parts of it are reflected at the interfaces. These reflected beams making constructive and destructive superposition and the resulting intensity of the light at different wavelength is detected. The interference depends on the thickness of the layer. For this reason very small changes in the thickness of the polymer layer are detectable.

Swelling in humid atmospheres

Two methods are used to determine the swelling behavior in situ in humid atmospheres.

A home-built flow-cell[10] was mounted at the sample stage of our M-44 ellipsometer. In the cell the samples were exposed to controlled humidity. For the generation and regulation of humid air an apparatus[16] operating with synthetic air (20.5% O_2 in N_2) and distilled water was used. Swelling was measured in the dynamic mode of spectroscopic ellipsometry at one angle of incidence (75°), the data points were collected every 12 seconds.

The same swelling experiments were done using Reflectometric Interference Spectroscopy[17]. From the in-situ interference spectra in the visible spectral range very small changes in the optical thickness of the HBP layers due to swelling can be calculated. The measurements were done at room temperature and a flow rate of 500 mL/min of synthetic air. The humidity is controlled by mixing dry and saturated gas flow.

Results and discussion

Properties of the films

Using the standard spin coating conditions described above, HBP layers of about 80 nm in thickness were formed with good reproducibility. The spin coating parameters had not as much influence on the thickness as the concentration of the HBP solution. For example 600 nm thick layers were prepared with a 10% (w/w) solution. The spin-coated layers are uniform and homogeneous looking at their lateral distribution. An ellipsometric mapping experiment measuring an array of points all over the coated surface gives values of thickness and refractive index within the standard error limits of the instrument. Fig. 2 shows the refractive index n as function of the wavelength for a carboxyl-terminated HBP. As expected for dielectric layers the refractive index of HBP decreases slowly with increasing wavelength. No optical absorption could be observed in the measured visible spectral range that means k (λ) = 0.

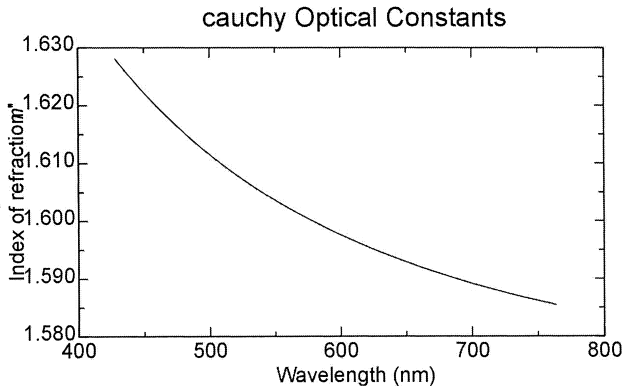

Fig. 2 Refractive index n of P-COOH in dependence on the wavelength

To show investigated differences between the HBP we extracted n at a standard wavelength λ = 630 nm from the spectral curves (Table 2).

It is known that the dielectric constant or refractive index of thin polymer films are affected by several factors as chain flexibility, molecular architecture and order and polarizibility of the chain segments and functional groups as well. Furthermore, layer density, free volume and the presence of additional components like water and/or solvent impurities play an important role.

Table 2 Refractive index n (630 nm) of HBP

HBP	n (630 nm)
P-OH	1.6342
P-COOH	1.5993
P-OAc	1.5815

Comparing our three types of investigated HBP a strong similarity in the linear and branched units, in molecular weight and of course in the layer preparation procedure is established. The linear aromatic ester segments are of the same nature. So the differences in the refractive index (Table 2) should be caused mainly by the terminal groups. The P-OAc has the lowest n value. As we know from the infrared spectra and thermogravimetric analysis, adsorbed water and hydrogen bonding have to be considered especially in the P-OH and P-COOH layers. In this case the higher n as effective medium value indicate a more compact structure and higher polarizibility.

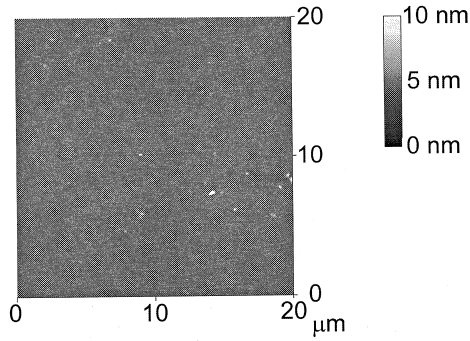

Fig. 3 Tapping-mode AFM height image of P-COOH

The topography of the HBP films on the silicon wafer was examined by atomic force microscopy. Fig. 3 shows a typical AFM height image obtained for P-COOH. Typical mean roughness values calculated from AFM images are in the range of several Angstroms on a μm length scale indicating very smooth HBP surfaces. In addition, scanning electron and optical microscopy also provide indications for very smooth surfaces.

In summary we can conclude from the ellipsometry and microscopy results that our spin-coated HBP films are very homogeneous, uniform and smooth.

The chemical structure of the HBP can be proved by infrared spectroscopy. The different end groups were clearly identified in the films and separated from the branched backbone units. The position and assignment of characteristic IR bands are shown in Table 3.

Table 3 IR data of HBP, separated in bands from backbone and end groups

Backbone		P-OH		P-COOH		P-OAc	
ν (C-H)$_{arom}$	3090 cm^{-1}	ν (OH)	3600-2600 cm^{-1}	ν (OH)	3600-2600 cm^{-1}	ν (C=O)$_{OAc}$	1770 cm^{-1}
ν (C-C)	1595 cm^{-1}	ν (C-O)	1280 cm^{-1}	ν(C=O)$_{COOH}$	1702 cm^{-1}	ν(C-O)	1274 cm^{-1}
ν (C=O)$_{ester}$	1739 cm^{-1}						
ν (C-C)	1440 cm^{-1}						
ν (C-O)$_{ester}$	1180 cm^{-1}						

While in a linear polymer the end groups often can not be detected, in hyperbranched polymers the signals are strong enough because of their high number. Furthermore, different types of association of the polar hydroxyl and carbonyl groups can be distinguised. For example the broad band in the carbonyl region of P-COOH (see Fig. 4) is formed as complex band by the C=O stretching vibrations of backbone ester groups (1742 cm^{-1}) and of the weak (1725 cm^{-1}) and strong hydrogen bonded carboxyl groups (1705 cm^{-1} and 1692 cm^{-1}), respectively. The hydrogen bonding effects together with water adsorption/desorption were investigated in detail by recording the IR spectra during heating/cooling cycles (25 °C to 200 °C). In this way band assignment and reversibility of the association were proved.

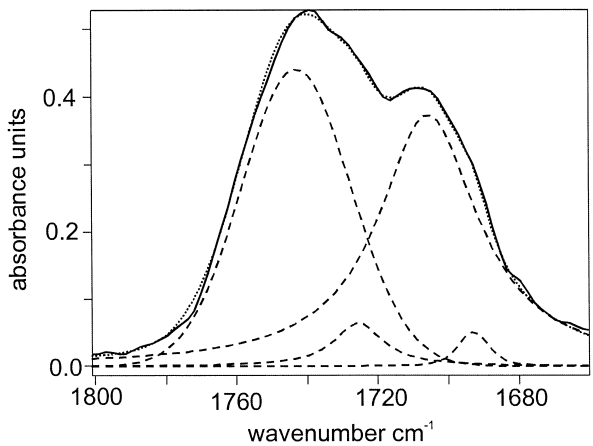

Fig. 4 Carbonyl bands of P-COOH with separation to several different vibrations
—— measured band ---- separated curves ····· sum of the separated curves

The remarkable sorption of water in P-OH and P-COOH is promoted by the hydrophilic character of the films. The occurrence of hydrogen bonding suggests a higher water affinity of the hydroxyl- and carboxyl-terminated polymers. The water content determined by thermo-gravimetric analysis (Table 1) verifies this presumption.

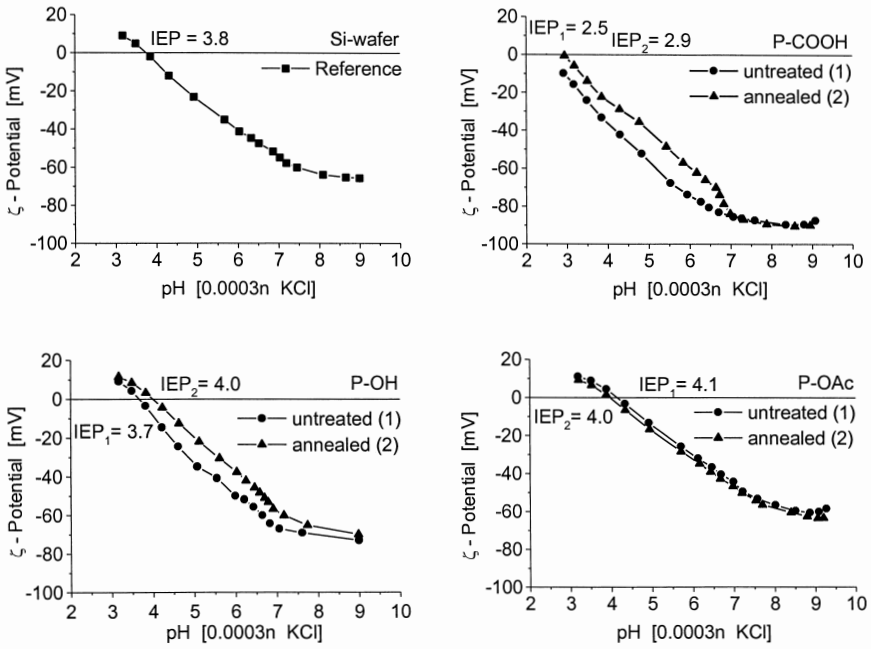

Fig. 5 Zeta potential of HBP surfaces as a function of the pH of the electrolyte solution

A very sensitive method to get indirect information about functional groups at the outermost surface of the films is the zeta-potential technique. Using the streaming potential method, the acidity or basicity of planar solid surfaces can be determined qualitatively from zeta potential versus pH plots. If the dissociation of functional groups is the predominant mechanism of double layer formation, the isoelectric point (IEP) (cf. Fig. 5) is a measure of the acidic or basic character of the solid surface. In the case of low IEP values, the solid surface possesses acidic functional groups, whereas IEP's in the alkaline pH range are an indication for basic functional groups at the outermost surface. As can be seen from the low isoelectric point obtained from the ζ versus pH plot (IEP: pH = 3.8), the bare silicon wafer has an acidic surface character due to the acidic silanol groups. Films of HBP P-OH (thickness: 80 nm) prepared on this silicon wafers show very similar ζ versus pH curves. The isoelectric point is reached at

pH = 3.7. Thus, the acidic surface character of P-OH is comparable with the acidic surface of the silicon wafer. In the case of P-COOH, the IEP value is shifted to lower pH values indicating the stronger acidic character of this surface (IEP: pH= 2.5).

Annealing of the P-OH and P-COOH films results in a change of the acidic character of the polymer surfaces and, hence, in the amount of acidic functional groups at the outermost surface. The IEP is shifted towards higher pH values (see Fig. 5). The decreasing amount of polar functional groups after annealing is thermodynamically favorable. As could be shown by contact angle measurements (see next section) the surface free energy is lowered after annealing. It is a well known phenomenon, that at temperatures above T_g, restructuring and reorientation of functional groups can occur due to the higher mobility of the polymer chains[18]. This behavior could not be observed in the case of P-OAc films. In contrast to the other two HBP´s, the IEP of the P-OAc film at pH = 4.1 was not shifted to higher values after annealing. In addition, this polymer surface shows the highest isoelectric point. Since polymer surfaces, possessing no dissociable functional groups, yield ζ versus pH curves very similar to the curve observed for P-OAc[19], the predominant mechanism of double layer formation is not yet clear in this case. Both, dissociation of functional groups as well as the preferential adsorption of hydroxyl (OH-) ions from the electrolyte solution can cause the observed curves for P-OAc shown in Fig. 5.

The surface properties of the HBP films have also been investigated using contact angle measurements based on axisymmetric drop shape analysis (ADSA). Typical contact angle patterns obtained by ADSA are shown in Fig. 6 for P-OH. As can be seen in this figure, four parameters were measured simultaneously: the drop volume, V, the three-phase contact radius, r, the contact angle, θ, and the liquid surface tension, γ_{lv}, of the sessile drop. In the specific example given in Fig. 6a the drop periphery was advanced at a rate of 0.343 mm/min. The constancy of the contact angles with increasing R indicates that θ is independent of the location of the contact line on the HBP surface. The advancing contact angles were averaged to yield a mean contact angle of $62.25° \pm 0.03°$. The error limit is the 95% confidence interval. Generally, four different, newly prepared films were used to calculate an averaged advancing contact angle for each HBP surface. These values are summarized in Table 4. From the advancing contact angles of water, the surface free energy of the different materials can be calculated using the equation-of-state approach[20]. The results show that films consisting of P-OH and P-COOH indicate hydrophilic surface properties. Both HBP have nearly the same surface free energy of about 46 mJ/m^2. This relatively high value is caused by acidic functional groups at the outermost surface as could be proved by the zeta potential measurements.

When these films are annealed above T_g, then the surface free energy drastically decreases to a value of about 30 mJ/m^2 (see Table 4) which is in accordance with the expected thermodynamically favored behavior. Hence, contact angle and zeta potential measurements, as well, show the change in the surface properties from a hydrophilic to a more hydrophobic HBP surface.

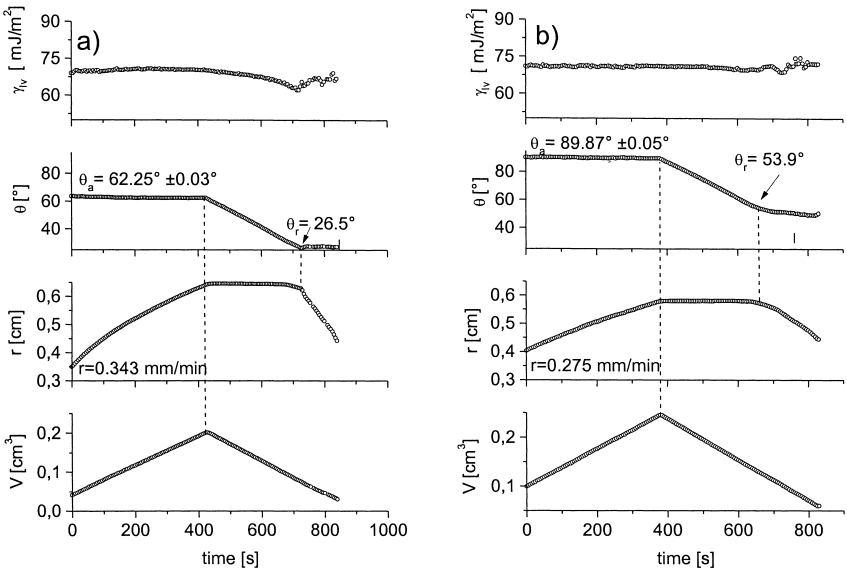

Fig. 6 Low-rate dynamic contact angles of water on P-OH surfaces measured by ADSA, a) untreated, b) annealed

As can be seen from Table 4, P-OAc surfaces are distinctly less hydrophilic with surface free energies of about 36 mJ/m^2. There is no change in the surface energetic properties due to annealing. Again, this result is in excellent agreement with the result obtained by zeta potential measurements for P-OAc.

In addition to the advancing contact angle, ADSA is also very suitable to quantify contact angle hysteresis by measuring receding contact angles when the liquid is withdrawn from the sessile drop (see Fig. 6). The receding contact angles shown in Table 4 are those values which can be measured when the three-phase contact line begins to retract. This point is marked in Fig. 6. It is remarkable that contact angle hysteresis is distinctly larger on the more hydrophilic P-OH and P-COOH surfaces than on P-OAc surfaces (see Table 4). Since all polymer surfaces are very smooth, it can be assumed that the lower hysteresis is due to a chemically more homogeneous surface.

Table 4 Summary of water contact angles on three different HBP surfaces. The surface free energy was calculated from the advancing contact angle using the equation-of-state approach[20)]

	advancing contact angle [°]	surface free energy γ_{sv} [mJ/m^2]*	receding contact angle [°]	contact angle hysteresis $\Delta\theta$ [°]	
P-OH	62.4 ± 0.5	46.0	25.3 ± 1.4	37.1	untreated
	88.4 ± 1.4	29.8	54.1 ± 1.6	34.3	annealed
P-COOH	61.1 ± 0.9	46.7	n.d.	n.d.	untreated
	87.6 ± 1.3	30.3	37.5 ± 1.2	50.1	annealed
P-OAc	77.2 ± 0.3	36.8	54.1 ± 1.3	23.1	untreated
	78.8 ± 1.0	35.8	59.4 ± 1.0	19.4	annealed

*γ_{lv} (H_2O) = 72.5 mJ/m^2

Swelling in humid atmospheres

The analysis data discussed above propose a high sensibility towards water especially for the hydroxy- and carboxylic-terminated samples, while the acetoxy-terminated sample should be more hydrophobic. Therefore the swelling behavior in humid air simulating very dry and wet conditions should be different for samples with different end groups.

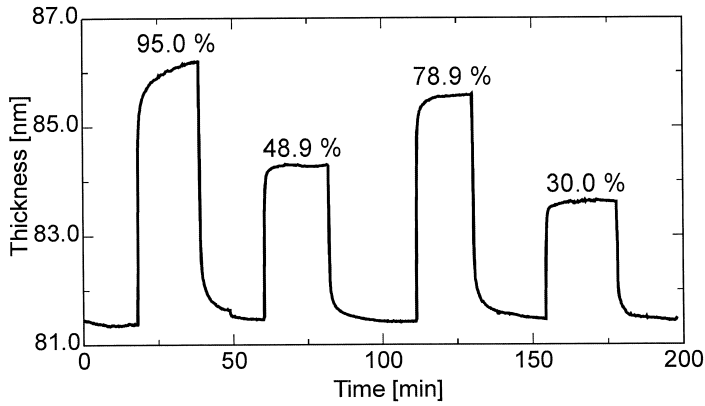

Fig. 7 P-OH In situ ellipsometry: film thickness is dependent on time under variation of the relative humidity

In Fig. 7 a typical result of in-situ ellipsometry is represented, which shows that the baseline is reproducible and stable over the measuring time. For the swelling process the equilibration

is rapid, while the de-swelling takes several minutes (at very high atmospheric humidity the humidity rises from 93.9 % to 95.0 % during the measurement. The equilibration is superposed with changes in humidity.)

The relative thickness increase is linear correlated to the relative humidity atmosphere (Fig. 8). The fitted refractive index versus the relative humidity should also show a linearity, but the changes are very small and within the error of the fitting process. Only for the highest measured relative humidity a trend to lower values is detectable.

Also the difference between the both hydrophilic to the hydrophobic polymer is obvious: The hydroxyl- and the carboxyl acid-terminated materials show an increase in thickness of about 7 % while the other swell only about 0.5 %. For verification different samples of the same material are exposed statistically to different humidities and the same value of swelling are detectable (Fig. 8). In comparison to other aromatic polymers applied as sensoric layers like aromatic polyimides, the swelling is very strong[21] whereas polyelectrolytes shows a stronger effect[7].

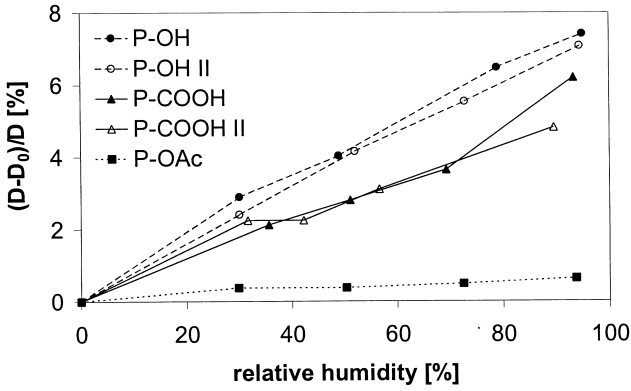

Fig. 8 Increasing film thickness in dependence of relative humidity, D_0 = initial thickness, D = equilibrium thickness, several sample types were monitored (P-OH; P-OH II, P-COOH; P-COOH II)

Independent measurements of relative changes in the optical thickness (nD) performed by RIfS were in agreement with the data of the spectroscopic ellipsometry (Fig. 9). The swelling of P-OH and P-COOH is again notable stronger as P-OAc and the magnitude is in the same range. The curves also demonstrate the reversibility of the water adsorption/desorption processes.

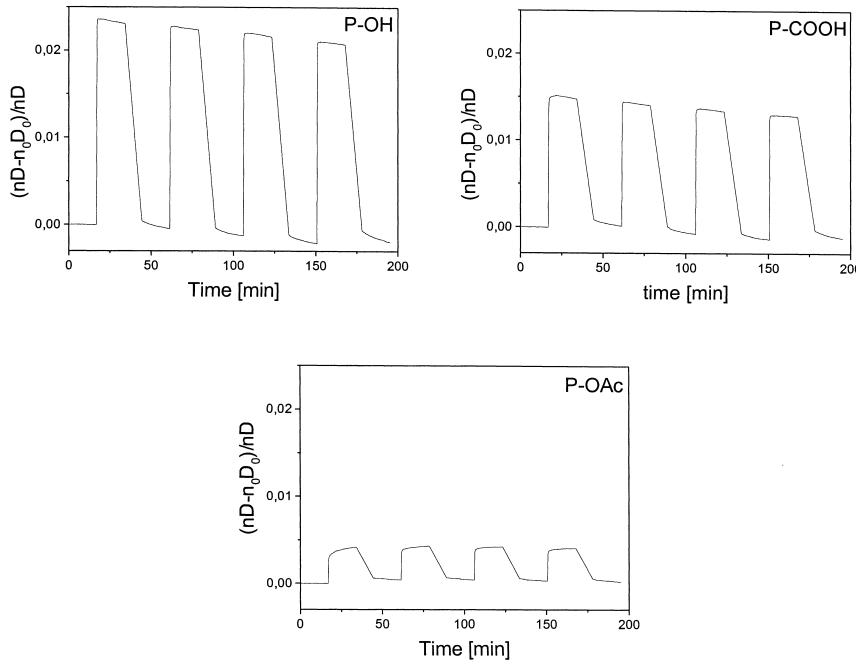

Fig. 9 Typical result for RIfS measurements on different HBP at 20% relative humidity (no baseline correction)

Conclusions

Isotropic thin films of HBP with a smooth surface can be easily prepared by spin coating. The surface properties of P-OH and P-COOH films were to be hydrophilic due to acidic functional groups at the outermost surface. When these films were annealed above T_g, the surface free energy decreases drastically. P-OAc surfaces are less hydrophilic and these surfaces do not change their surface properties after annealing.

These differences in molecular structure and surface properties result in differences in the swelling behavior in atmospheric humidity. The hydrophilic HBPs show a strong effect in contrast to the less hydrophilic P-OAc. The polarity of the surface should have a strong influence on the swelling process. From these result we can expect that hyperbanched polymers with different end groups swell selectively in volatile organic compounds (VOC) with different polarities. Thus this kind of HBP films seem to be an interesting material for chemical sensors.

Acknowledgments
The support of this work by Deutsche Forschungsgemeinschaft within the Sonderforschungsbereich 287 is gratefully acknowledged.
The authors thank A. Janke (AFM) and C. Werner (Zeta potential) for technical support and helpful discussions. The authors also gratefully acknowledge support of the work by M. Herold (Tübingen University).

---

[1] B. Voit, J. Polymer Sci. A, Polymer Chemistry **38**, 2505 (2000)
[2] Chemical and Engineering News, June 3, 1996
[3] H. Tokuhisa, R. M. Crooks Langmuir **13**, 5608 (1997)
[4] H. Tokuhisa, M. Zhao, L. A. Baker, V. T. Phan, D. L. Dermody, M. E. Garcia, R. F. Peez, R. M. Crooks, T. M. Mayer J. Am. Chem. Soc. **120**, 4492 (1998)
[5] M. L. Bruening, Y. Zhou, G. Aquilar, R. Agee, D. E. Bergbreiter, R. M. Crooks Langmuir **13**, 770 (1997)
[6] H.Tokuhisa, R. Peez, D. L. Dermody, R. M. Crooks Photochemistry and Photobiolgy **65,** 96 (1997) (Abstract of the 25th Annual Meeting of American Society)
[7] M. Biesalski, J. Rühe Langmuir **16**, 1943 (2000)
[8] a) D. Schmaljohann „Funktionalisierung von hochverzweigten Polyestern für den Einsatz als Beschichtungs- und Blendmaterial" Herbert Utz Verlag, Wissenschaft, München 1998 b) B. Voit, S. R. Tuner, T. Mourey Macromolecules **26**, 4617 (1993) c) S. R. Tuner, F. Walter, B. Voit Macromolecules **27**, 1611 (1994)
[9] a) C.J. Hawker, R. Lee, J. M. J. Fréchet J. Am Chem. Soc. **113**, 4583 (1991) b) K. L. Wooley, C.J. Hawker, R. Lee, J. M. J. Fréchet Polymer J. **26**, 187 (1994) c) K. L. Wooley, C.J. Hawker, R. Lee, J. M. J. Fréchet Polymer J. **26**, 187 (1994)
[10] C. Werner, K.-J. Eichhorn, K. Grundke, F. Simon, W. Grählert, H.-J. Jacobasch, Colloids and Surfaces Part A: Physicochem. and Engineering Aspects **156**, 3 (1999)
[11] S. Schwarz, K.-J. Eichhorn, E. Wischerhoff, A. Laschewsky Colloids and Surfaces Part A: Physicochem. And Engineering Aspects **159** (1999) 491-501
[12] a) H.-J. Jacobasch, J. Schurz, Prog. Colloid Polym. Sci. **77,** 40 (1988) b) H.-J. Jacobasch, Prog. Org. Coat. **17,** 115(1989)
[13] S. Lahooti, O. I. del Rio, P. Cheng , A. W. Neumann "Axisymmetric Drop Shape Analysis" In: A.W. Neumann, J.K.Spelt (eds) "Applied Surface Thermodynamics", Dekker, New York, (1996) 441-507
[14] P. Cheng, D. Li, L. Boruvka, Y. Rotenberg, A. W. Neumann Colloids and Surfaces **151** (1990)
[15] D. Y. Kwok, T. Gietzelt, K. Grundke, H. J. Jacobasch, A. W. Neumann Langmuir **13,** 2880 (1997)
[16] R. Buchhold, A. Nakladal, G. Gerlach, K. Sahre, K.-J. Eichhorn, M. Müller, Microsystem Technologies **5**, 3 (1998)
[17] F. Rathgeb, G. Gauglitz, Analytica Chimica Acta **372**,333 (1998)
[18] J. D. Andrade, L. M. Smith, D. E. Gregonis "The contact angle and interface energetics", in: "Surface and Interfacial Aspects of Biomedical Polymers" (Ed. J. D. Andrade), Plenum Press, New York (1985), vol. 1, ch. 7, 249-292
[19] K. Grundke, H.-J. Jacobasch, F. Simon, S. Schneider, J. Adhes. Sci. Technol. **9,** 327 (1995)
[20] J. K. Spelt, D. Li "The equation of state approach to interfacial tensions" in: "Applied Surface Thermodynamics" (Eds. A. W. Neumann, J. K. Spelt), Surfactant Science Series **63**, Marcel Dekker, New York (1996), 239-292
[21] R. Buchhold, A. Nakladal, G. Gerlach, K. Sahre, M. Müller, K.-J. Eichhorn, M. Herold, G. Gauglitz J. Electrochem. Soc. **145**, 4012 (1998)